# fMRI-Based Robotic Embodiment: Controlling a Humanoid Robot by Thought Using Real-Time fMRI

Ori Cohen, Sébastien Druon, Sebastien Lengagne, Avi Mendelsohn, Rafael Malach, Abderrahmane Kheddar

**Ori Cohen***
The Interdisciplinary Center
Herzliya 46150, Israel
and
Bar-Ilan University
Ramat-Gan 52900, Israel

**Sébastien Druon**
**Sébastien Lengagne**
CNRS-UM2 LIRMM UMR 5506
34095 Montpellier
Cedex 5, France

**Avi Mendelsohn**
**Rafael Malach**
Weizmann Institute of Science
Department of Neurobiology
Rehovot 76100, Israel

**Abderrahmane Kheddar**
CNRS-UM2 LIRMM UMR 5506
34095 Montpellier
Cedex 5, France
and
CNRS-AIST
Joint Robotics Laboratory
UMI3218
305-8568 Tsukuba, Japan

**Doron Friedman**
The Interdisciplinary Center
Herzliya 46150, Israel

# fMRI-Based Robotic Embodiment: Controlling a Humanoid Robot by Thought Using Real-Time fMRI

## Abstract

We present a robotic embodiment experiment based on real-time functional magnetic resonance imaging (rt-fMRI). In this study, fMRI is used as an input device to identify a subject's intentions and convert them into actions performed by a humanoid robot. The process, based on motor imagery, has allowed four subjects located in Israel to control a HOAP3 humanoid robot in France, in a relatively natural manner, experiencing the whole experiment through the eyes of the robot. Motor imagery or movement of the left hand, the right hand, or the legs were used to control the robotic motions of left, right, or walk forward, respectively.

## 1 Introduction

This work aims at dissolving the boundary between the human body and surrogate representations in immersive virtual reality and physical reality. By dissolving the boundary, we mean that the subject is expected to have the illusion that his or her surrogate representation is his or her own body, and behave and think accordingly. This may help disabled humans to control an external device just by thinking, without any bodily movement being involved. As illustrated in Figure 1, our aim was to provide a subject the most intuitive thought-based control of a robotic body. The subject was located in Israel and the robot was located in France; this geographic split was made due to the availability of the facilities. In order to reach this goal, we decided to focus on motor control, using real-time functional magnetic resonance imaging (rt-fMRI) to detect the subjects' movement intentions and translate them into actions performed by a HOAP3 humanoid robot.

The majority of brain–computer interfaces (BCIs) with humans are based on electroencephalogram (EEG) technology. Although fMRI is expensive and less accessible, fMRI-based BCI is promising for several reasons. The superior spatial resolution, as compared with EEG, may allow exploring new modes of BCI, based on new types of mental patterns. If successful, attempts can be made to localize underlying brain patterns with the fMRI and detect the same patterns using more accessible devices such as EEG or functional near-infrared spectography (fNIRS). The latter is especially relevant, since it is based on the same hemodynamic responses as measured by fMRI. fMRI-based BCI can also

*Correspondence to orioric@gmail.com.

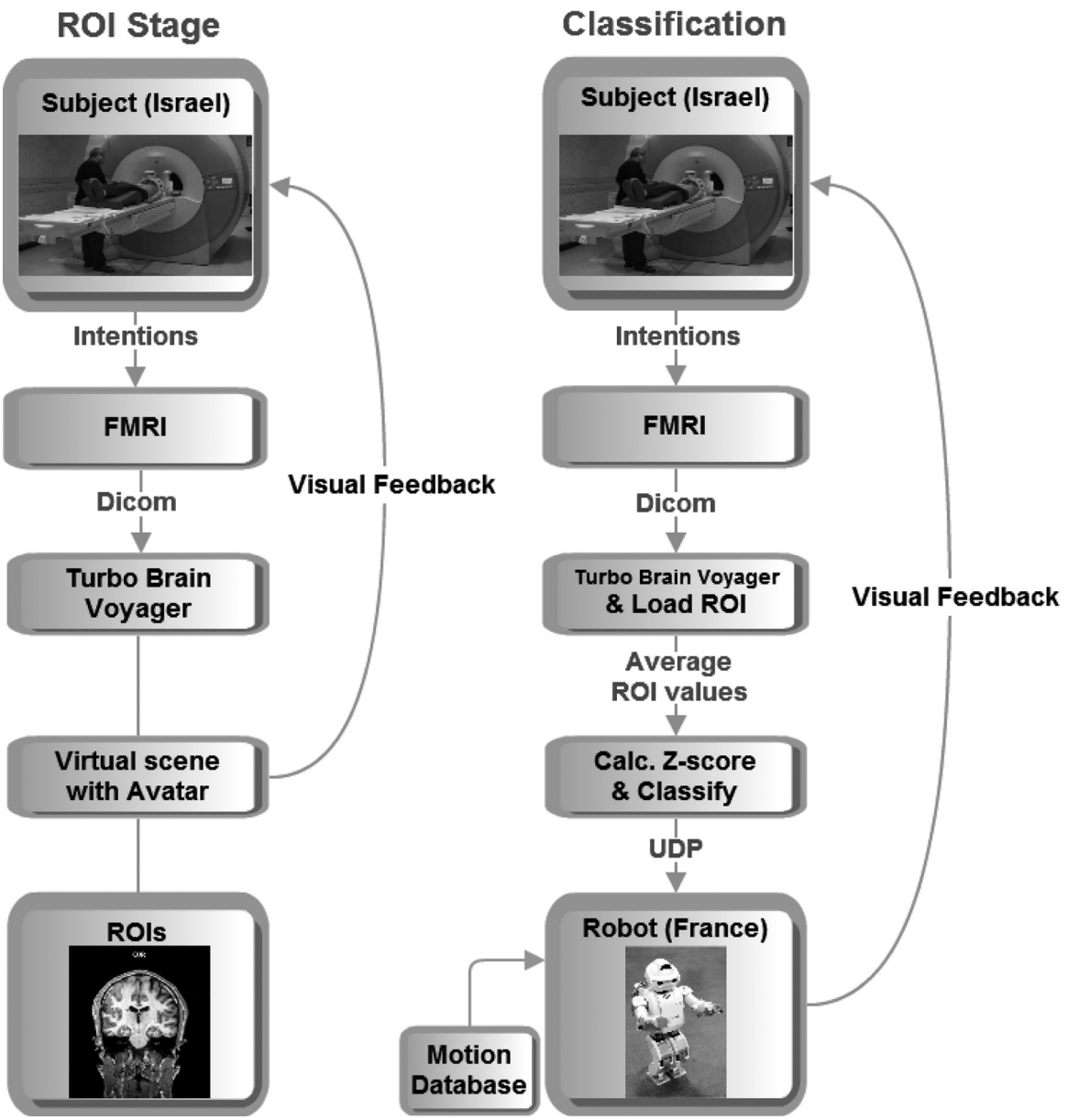


**Figure 1.** *Robotic embodiment: General principle of data processing and experimental tasks.*

be used for training patients in BCI, for rehabilitation sessions, or for next generation neurofeedback—in all these cases very specific brain areas may be targeted. Finally, smaller and portable fMRI devices may become available.[1]

1. http://www.news-medical.net/news/2008/07/08/39842.aspx

## 2 Previous Work

Telerobotics is the technology that allows a human operator to steer robots at a distance. Telerobotic control strategies have evolved from the classical master-slave control to advanced supervisory control (Sheridan, 1992). Shared autonomy and the sophistication of the robotic control allows a telerobot to be steered by

classical and modern input devices (such as keyboard, mouse, eye tracker, voice recognition system, etc.), or through a virtual reality functional intermediary (Kheddar, 2001). Recently, the possibility of using BCIs to control robots is gaining popularity. BCIs allow a human to control a computer or a mechatronic device just by thinking, without any body movement being involved. While contemporary BCI systems are far from the interfaces imagined by Hollywood in movies such as *Avatar*[2] or *Surrogates*,[3] there has been some progress made and a surge of interest in recent years (Mak & Wolpaw, 2009).

Most BCI research is aimed at helping paralyzed patients, such as patients with amyotrophic lateral sclerosis (ALS) and severe nervous system damage including spinal cord injuries and stroke, and the goal is to provide such patients with some level of communication, control of external devices, and mobility.

BCI was successfully demonstrated with invasive methods such as electrocorticography (ECoG, e.g., Leuthardt, Schalk, Wolpaw, Ojemann, & Moran, 2004) and intracortical neural interfaces (e.g., Donoghue, Nurmikko, Black, & Hochberg, 2007; Kim et al., 2011). Recently, a tetraplegic patient was able to use such electrodes to drink coffee by partially controlling a robotic arm (Hochberg et al., 2012). Most BCI systems intended for humans rely on the measurement of an EEG recorded from the scalp. BCI-controlled robots have primarily been demonstrated using three major EEG-based BCI paradigms: the Steady-State Visually-Evoked Potential (SSVEP), the P300 wave, and motor imagery.

In SSVEP, a flickering visual stimulus is displayed to the subject. When the retina is excited by a signal ranging from 3.5 to 75 Hz, the brain generates electrical activity at the same frequency as the visual stimulus, which can be detected in the EEG signal. SSVEPs are highly interesting for robot control due to their simplicity, their superior signal-to-noise ratio, and their high decision rate. Previous studies have explored its use in the control of mobile robots (e.g., Prueckl & Guger, 2009; Ortner, Guger, Prueckl, Graenbacher, & Edlinger, 2010), and recently, humanoid robots as well (Gergondet et al., 2011; Gergondet, Kheddar, Hintermuller, Guger, & Slater, 2012).

The P300 wave is an event-related potential (ERP) that appears 300 ms after an infrequent task-related event. This ERP is now commonly used in BCI systems due to its reliability: the waveform is easily and consistently detectable, with little variation in measurement techniques. Even though the bit rate (i.e., the amount of commands that are sent to the external object in a second) is typically lower than SSVEP, it is still a reliable BCI pattern, included in several robotic control systems (e.g., Bell, Shenoy, Chalodhorn, & Rao, 2008; Rebsamen et al., 2006; Iturrate, Antelis, Kübler, & Minguez, 2009; Rebsamen et al., 2010; Lenhardt & Ritter, 2010).

Because they rely on visual evoked responses, both SSVEP and P300 can be compared to eye-tracking systems in terms of input interface: they provide the same set of functionalities to the user and suffer from the same limitations. Mostly, the mapping between the user intentions and the functionality is arbitrary, in contrast to what we would expect from a thought-based interaction paradigm.

Motor imagery has also been used for EEG-based BCI. Motor imagery is a mental process by which an individual rehearses or simulates a given action. As explained in Neuper and Pfurtscheller (2001), imagination of movement evokes brain networks that are similar to the networks evoked by real execution of the corresponding physical movement. A series of studies was carried out with motor-imagery-based navigation of highly-immersive virtual reality (Friedman, Leeb, Pfurtscheller, & Slater, 2010; Pfurtscheller et al., 2006; Leeb et al., 2006) including experiments with a tetraplegic patient (Leeb et al., 2007). Royer, Doud, Rose, and He (2010) demonstrated navigating a virtual helicopter using four classes: right hand to move right, left hand to move left, both hands to move up, and none to move down. Motor imagery requires more training and the bit rate is lower than P300 and SSVEP, but it is arguably based on a more intuitive mapping between the mental patterns and the resulting action taken by the system.

2. http://www.imdb.com/title/tt0499549/
3. http://www.imdb.com/title/tt0986263/

Since an EEG is recorded at the scalp, it suffers from high levels of noise and low spatial resolution as compared with other methods for recording brain activity. fMRI also has several drawbacks: it is expensive, less accessible, and has low temporal resolution and a built-in delay because it is based on metabolic changes rather than on direct recording of electrical activity in the brain. However, due to its superior spatial resolution covering the whole brain simultaneously, it holds much promise for completely new types of control paradigms.

Real-time fMRI has been suggested for various applications (deCharms, 2008). Typically, rt-fMRI is used as a form of neurofeedback; that is, the raw signal values from a specific brain region are visualized on the screen, either as a bar or as a time-course plot, in order to provide immediate feedback (Weiskopf et al., 2003) or delayed feedback (Weiskopf et al., 2004). The subject uses a mental strategy to increase or decrease the activity in the target brain region. Such neurofeedback sessions are different from BCI in various ways. First, the goal is different: in neurofeedback, the goal is to train the subject to modulate his or her brain activity, whereas in BCI, the goal is to allow a subject to control an external device by thought. Most notably, in neurofeedback, most of the effort is done by the subject, and the system is used only for visualizing the brain signals, whereas BCI systems include algorithms for processing the brain signals and mapping them into specific actions taken by the external device. fMRI was used as an input device for robotic hand control as publicized by Honda Research Institute and Advanced Telecommunications Research (ATR); this nonpublished result was reported by Honryak (2006).

In traditional fMRI experiments, we collect data from a subject's brain and have abundant time after the experiment is complete to analyze the brain data. Additionally, algorithms do not need to be optimized for speed and for memory usage. Conversely, when dealing with real-time analysis and classification, we need to use fast algorithms that can manipulate large data sets in a fraction of a second. In our case, the time between repetition times (TRs), which is the time between our inputs, is 2 s. In the current real-time experiments, only three average raw values are calculated for the classification, so one of the advantages of the simplicity of our method is its computational efficiency.

## 3 fMRI-Based BCI

Our system is able to automatically identify a subject's intention based on motor imagery in real time, classify brain activation patterns, and convert them into robotic actions performed by a humanoid robot. The aim is to allow intuitive BCI control based on brain activity. This section describes the system and method used in the study.

### 3.1 The System

Imaging was performed on a 3T Trio Magnetom Siemens scanner, and all images were acquired using a 12-channel head matrix coil. Three-dimensional T1-weighted anatomical scans were acquired with high-resolution 1-mm-slice thickness (3D MP-RAGE sequence, TR 2,300 ms, TE 2.98 ms, 1 $mm^3$ voxels). For blood-oxygenation-level-dependent (BOLD) scanning, T2*-weighted images using echo planar imaging sequencing (EPI) were acquired using the following parameters: TR 2,000 ms, TE 30 ms, flip angle 80°, 35 oblique slices without gap, 20 toward coronal plane from anterior commissure–posterior commissure (ACPC), $3 \times 3 \times 4$ mm voxel size, and covering the whole cerebrum.

The data coming from the fMRI scanner is saved as Dicom files,[4] and processed by Turbo BrainVoyager software (TBV; Turbo Brain Voyager, Netherlands, n.d.), which is a real-time processing, analysis, and visualization application that accepts input from an fMRI scanner. After processing the data, TBV saves the average raw data values for each region of interest (ROI) selected by the operator at each measured time point.

The fMRI scanner is located in Rehovot, Israel, and the robot in Béziers, France. The flow of high-level commands (forward, left, right) was sent to the robot through a User Datagram Protocol (UDP) connection

4. http://medical.nema.org/

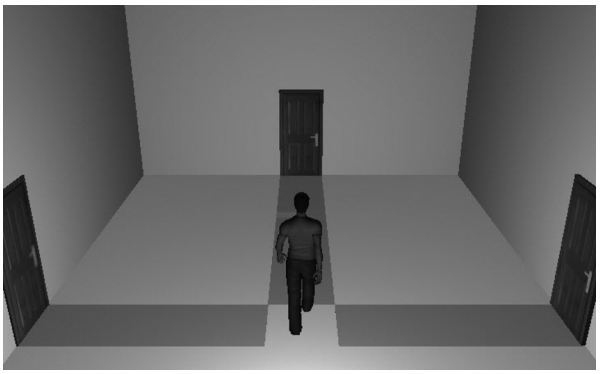

**Figure 2.** *The subject sees an avatar in the center of a three-door room. The subject hears an auditory command and needs to use motor imagery or movement that corresponds to it.*

and the video flow was received through another network flow. The round-trip time from transmission to reception of data (ping) between Israel and France was between 100 to 150 ms. Similar to many teleoperation systems, the vision flow is critical. While a dropped frame may not be perceived by the fMRI user, the latency must be as low as possible. We used the visionsystem framework[5] to acquire, transcode, and transmit the video flows.

### 3.2 The ROI-Based Paradigm

Each experiment is divided into three parts. The first part is intended for localization of brain areas: the subject sees an avatar standing in the center of a three-door room, as seen in Figure 2. The subject is given pseudorandom instructions and is expected to follow them. After each action, the subject is instructed to rest, and during that time, the avatar executes a predetermined command that corresponds to the instruction. The "right" and "left" commands result in the avatar turning toward the right or left door correspondingly, and the "forward" command results in the avatar moving toward the top door. The total amount of instructions is divided equally between all instruction types. The entire session is recorded for the purpose of finding ROIs. An ROI is a selected group of voxels

5. https://github.com/LIRMM-Beziers/visionsystem

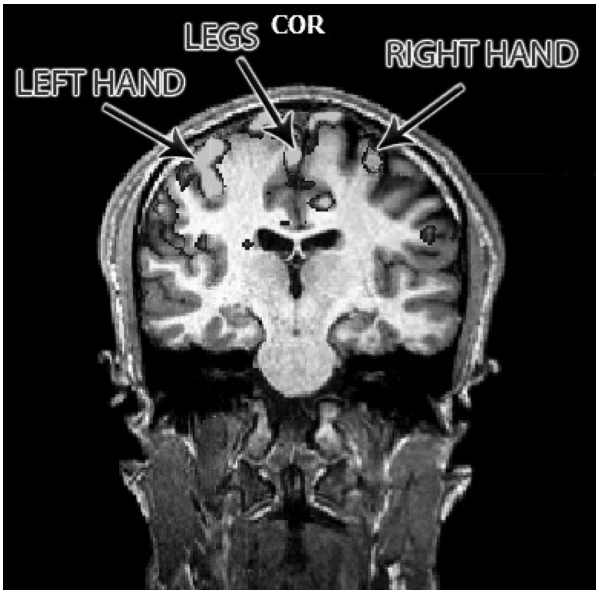


**Figure 3.** *An example of right-hand versus left-hand contrast and legs versus baseline contrast, taken from one subject over the first stage of the experiment, intended for localization of ROIs.*

in the brain; in our study, we select a group of voxels that were more active in one experimental condition compared to the other condition, as detected by a General Linear Model (GLM). The experimenter manually marks the ROIs inside the bright areas of the relevant anatomical regions where the event-related average signal for the current ROI is significantly higher than the other two ROIs. Figure 3 depicts an image from TBV's view screen. The three regions (from left to right) represent the three areas correspondingly: left hand, legs, and right hand, in the primary motor cortex, and are delineated by a left versus right hand contrast as well as a legs versus baseline contrast, using a GLM analysis. Figure 4 depicts the event-related average time-course of the contrast. We assume that there are intersubject differences in the specific ROIs; however, these ROIs are always expected to be found in the primary motor area and are easy to locate with the GLM contrast (this may be inconvenient to reproduce in other studies, but we are already improving our system to use an automated method).

In the second part, we instruct the subject to rest for 1 min; this serves as a baseline resting period in which

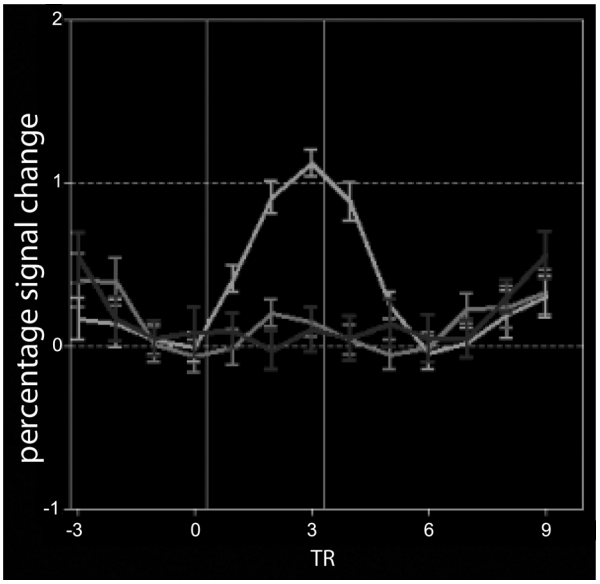


**Figure 4.** *An example of event-related averaging plot for left-hand ROI, taken from one subject. This plot depicts the average hemodynamic response evoked by the stimulus for an ROI over the first phase of the experiment. X and Y axes represent the TR position corresponding to the beginning of the event and the percentage signal change, respectively.*

we collect the mean and standard deviation for each ROI for the entire baseline period.

In the third and last part, the task stage, we instruct the subject to imagine moving his or her limbs and collect the average values from each ROI every 2 s. A classification is made using the $z$-score formula and is calculated for each measured value by using the mean and standard deviation from the baseline period:

$$z = \frac{x - \mu}{\sigma}, \tag{1}$$

where

- $x$ is the average raw value in an ROI in the current TR;
- $\mu$ is the mean raw value of the ROI in the baseline period; and
- $\sigma$ is the standard deviation value of the ROI in the baseline period.

The selected class at each time step is the class corresponding to the ROI with the maximal $z$ score value for that duration. The system then transmits the classification to the HOAP3 robot located in France. Each ROI is mapped to a different action performed by the subject, which in turn activates a precomputed robotic motion. Turning left, right, or walking forward corresponds to left-hand, right-hand, or legs imagery, respectively.

### 3.3 Generation of the Motion Database for the Robot

In order to control the robot through such high-level instructions, we created a motion database for a follower task with the HOAP3 robot. Contrary to human-sized robots, small humanoid robots such as HOAP3 are very stable. Hence, we are free to execute those motions with a local joint control loop, without using a balance stabilizer. Moreover, the robot receives a new command every 2 s and has to walk on a flat floor without obstacles. Thus, there is no need for a reactive pattern generator, and the use of a motion database is fairly straightforward in our case for producing tasks such as tracking as presented in Lengagne, Ramdani, and Fraisse (2011). In this paper, we use the method presented in Lengagne, Vaillant, Yoshida, and Kheddar (2013) to generate motions performing a sequence of contact stances and to ensure the balance and the physical limits of the robot.

Video feedback to the user is obtained directly from the HOAP-3 embedded cameras.

### 3.4 Motion Optimization

As presented in Lengagne et al. (2013), the goal is to compute the joint trajectories $q(t)$ that minimize a cost function $C$, perform the desired task, and ensure the integrity of the robot.

$$\begin{aligned} &\min_{q(t)} && C(q(t)) \\ &\text{subject to} && \begin{cases} c_{\text{eq}}(q(t)) = 0 \\ c_{\text{ineq}}(q(t)) \leq 0 \end{cases}, \end{aligned} \tag{2}$$

where $c_{\text{eq}}$ is the set of continuous equality constraints that allows for the definition of the foot position during a contact phase, and $c_{\text{ineq}}$ is the set of continuous inequality constraints relative to the balance and the

limits of the robot. In order to deal with the constraints, classical optimization techniques revert to time discretization, even if they may produce unsafe motions, where some constraint violations between the instants of the time-grid may occur, as shown (Lengagne et al., 2011). In order to avoid any constraint violation, this method considers a time-interval discretization that decomposes the motion into several intervals and uses a polynomial approximation over each time interval of any state variables of the robot, in order to easily take into account continuous inequality and equality constraints.

### 3.5 Motion Properties

We created a database of motions in order for the robot to walk forward, turn to the left, or turn to the right. Each motion is decomposed into several contact phases, that is, a lapse of time when no contacts are created or released. To ensure continuity, every motion starts and ends with the same posture. The turning motions are composed of five phases that perform a rotation of 30°, whereas the walking motions are composed of nine phases that produce steps of 5 cm each.

During the optimization processes, we considered the following cost function that produces a smooth and low-energy motion:

$$C(q) = a \int_0^T \sum_i \Gamma_i^2 dt + b \int_0^T \sum_i \ddot{q}_i^{\,2} dt + cT, \quad (3)$$

where $a = 1e-2, b = 1e-5$, and $c = 4$ are the values we set heuristically to have human-like walking motion (from Lengagne et al., 2013).

## 4 Experimental Validation

### 4.1 Experimental Setup

In a parallel work (Cohen, Koppel, Malach, & Friedman, 2014), we consider the same ROI paradigm applied to the control of a virtual avatar—while in this work, we deal with the control of a physical robot. In the study reported here, we also used the avatar as a feedback in the first experimental stage, which was intended for defining three nonintersecting ROIs per subject. The subjects saw a virtual environment with an avatar standing in the bottom center of the space, and were instructed to imagine themselves as the avatar. The avatar would turn 90° toward either the left or the right, or would walk 2 s when facing forward. In BCI, we would like to achieve the most intuitive mapping between thought patterns and the resulting interaction (Friedman et al., 2010). Imagining hands for motion direction and feet for forward motion is not identical to the way you control your body when walking, but it is clearly not arbitrary or intuitive.

In the next step, the subjects viewed a live video feed through a camera located at the eyes of the robot. The robot was located inside a 9.6 × 5.3 m room in France. The participants saw a technician who instructed them to move left, right, or forward using hand gestures. This method also allows the researchers to assess that the robot motion truly reflects the thought-based instructions initiated by the subject. The objective given to the subjects in this experiment was to walk around two obstacles in a figure-eight-shaped course, for an approximate length of 1.5 m. Each subject underwent between three and seven test sessions, each lasting 12 min (360 TRs), in which the BOLD signal from the entire brain was measured every 2 s. At the end of this period, we calculated two values: the mean signal and the standard deviation for the entire rest period.

The system sent a nominal value to the robot every 2 s (corresponding to the ROI with the maximal $z$ score). The left or right commands initiated a 30° turning sequence, and the forward command initiated a two-step forward walking sequence, both lasting between 8 and 14 s. The robot executed a new command only after completing the previous command; that is, many of the commands classified by the system were ignored by the robot, and in practice the robot performed between 25 and 45 commands per session. In practice, while each command was based on a 2-s time window, the subjects focused on the same command (left, right, or forward) for the time it took the robot to perform the

action, which was longer. One alternative is to average the BOLD signal over the time it takes the robot to complete an action. However, due to the hemodynamic delay, we expect these latter values to be the "best" ones; we chose to allow the BOLD signal to reach its peak and stay at a relatively constant plateau during the time window of the robot action.

### 4.2 Subjects

The study included four right-handed participants: one man (age 26), referred to as S1, who performed 10 successful sessions of 12 min, using either exclusively motor imagery or motor movements, and three women (ages 25, 28, and 33) who performed the task using motor movements.

We tested the system with both motor imagery and motor movement; in the latter case, subjects were instructed to move their fingers and toes in order to move, rather than the corresponding imagery tasks. Because the commands are only extracted from brain signals, and because eventually such interfaces are intended for paralyzed patients, allowing the subjects to move their fingers and toes is still of interest. When using imagery alone, we occasionally fit the subject with electromyography (EMG) sensors on his or her hands and legs, and verify there is no electrical activity sent to the muscles. This test was done with S1 on other occasions when controlling the avatar by thought, but due to time constraints, this test was not done in the current study. S1 had participated in many motor imagery sessions previous to this study, had complete control of all three imagery commands, and therefore was the only subject selected to perform the task using motor imagery.

In the case of motor movement, the resulting brain signal and contrast are relatively strong; our experience indicates that any subject can perform the task without any difficulty and with literally no training. However, using motor imagery, the subjects need to be trained for several two-hour sessions. The training is necessary because it takes time for the subject to find the right imagery strategy to activate the motor regions. For example, participants imagine tapping with either right or left hand to turn, and imagine moving their feet back and forth to walk forward.

## 5 Results

Free-choice scenarios allow for an experience of performing a task in a relatively natural and continuous mode, as opposed to trigger-based BCI experiences. A limitation of free-choice scenarios is that it is difficult to accurately measure success rates. We have obtained accuracy measures from S1 of the same method with an avatar-based experiment; these were 100% for a two-class (50% chance-level) task (right hand vs. left hand) and 93% for the three-class (33% chance-level) task, across several runs, using the same ROI-based method as reported here (Cohen, Druon, Lengagne, Mendelsohn, Malach, Kheddar, & Friedman, 2012). In our experiment, the subject was always successful in performing the task in the allocated time. However, different subjects had various degrees of control, and some completed the tasks faster than others. Most trials were constructed so that time allowed for errors. In the present scenario, the subject was able to surround both obstacles by following visual instructions made by the technician. We cannot quantify success rates, but it is clear that the probability of successfully completing the 12-min task with chance-level control is extremely small. We tested the same method by allowing subjects to guide a 3D avatar following a trajectory on a virtual path. Seven subjects were able to perform the task with a high level of success; the results will be published elsewhere.

The participants were asked to perform one of the following three missions.

- **Free Navigation.** The user is allowed to visit the room freely.
- **Seek and Find.** An operator shows an object to the robot, then hides it. The subject has to navigate the room to locate it.
- **Follower.** An operator indicates (by gestures to the robot) the path that should be followed. This figure-eight-shaped path wound around two obstacles in order to use all of the three basic movements.

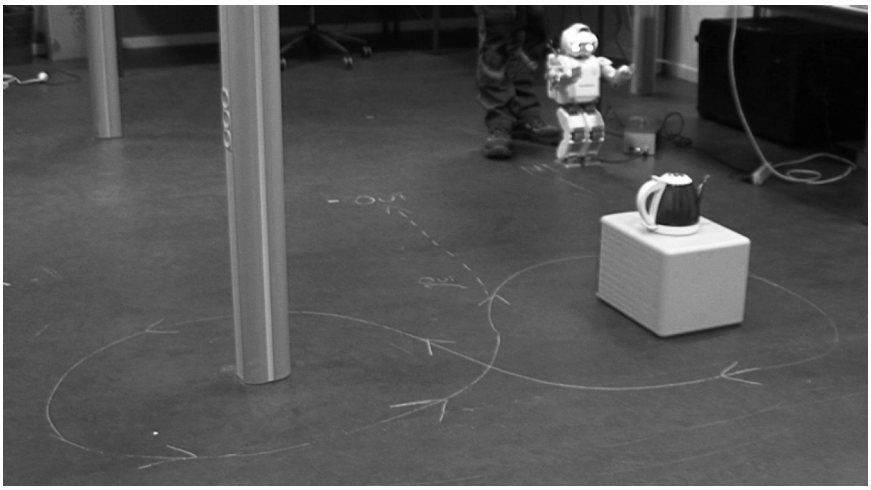

**Figure 5.** *The lab room in France, in which the figure-eight-shaped path was drawn on the floor.*

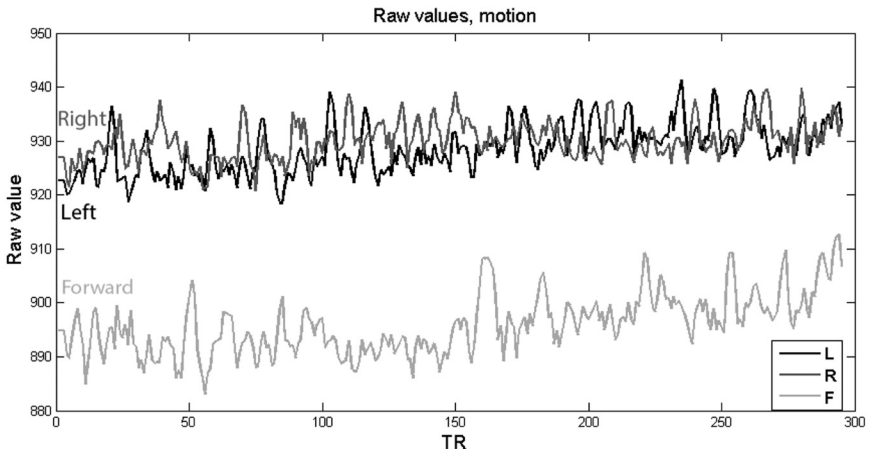


**Figure 6.** *Raw BOLD activation levels of subject S1 in the three ROIs used to control the robot with motion (fingers and toes).*

In one of the runs, S1 successfully completed the figure-eight-shaped path, shown in Figure 5, by reaching the out point in exactly 12 min.

Figures 6–11 show the mean activation values of the three ROIs over two sessions performed by subject S1 from two sessions: in one session the subject was allowed to move both fingers and toes, and in the other session the subject only used motor imagery. Figures 6–7 show the raw values for the three conditions in both motor movement and motor imagery. In order to classify the subject's intentions, we normalized the raw BOLD values using the *z* score formula and choose the highest signal as the classified action, as shown in Figures 8 and 9.

During the baseline duration (30 TRs), all three regions fluctuated synchronously (Figures 10 and 11). In contrast, the task phase (Figures 8 and 9) is composed of sections such that in each section one of the ROIs has increased activity compared to the other two ROIs that typically remain in sync: this is the result of the subject activating one of the three motion types (by either imagery or motion) selectively in order to control the robot. The switch among regions (classes) is relatively slow. In this case, the robot itself was slow

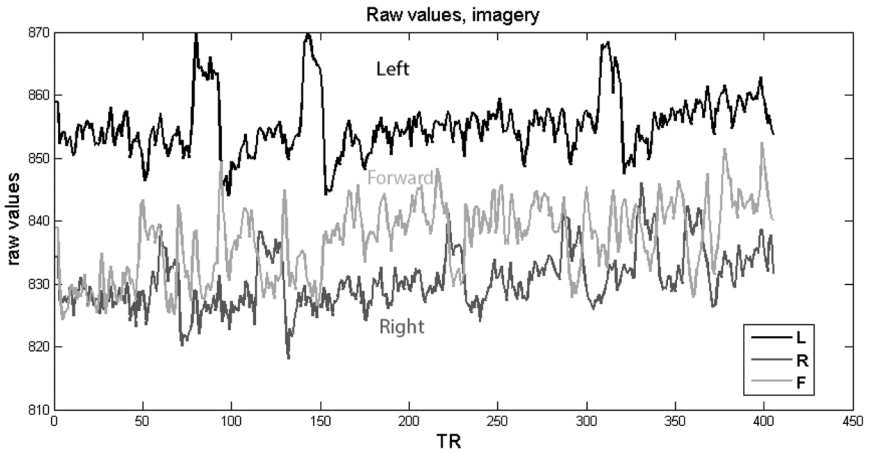


**Figure 7.** *Raw BOLD activation levels of subject S1 in the three ROIs used to control the robot with motor imagery.*

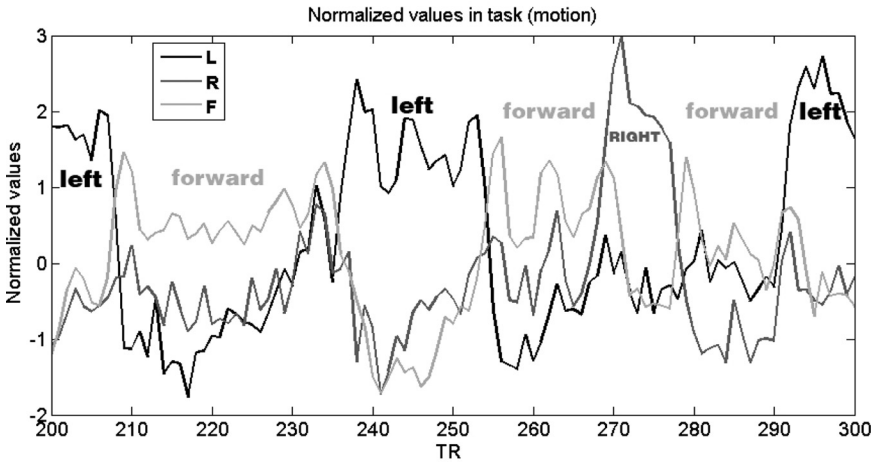


**Figure 8.** *Normalized activation levels of subject S1 in the three ROIs used to control the robot, during task, using motion.*

and took a few seconds to move forward or rotate. In future work, we will examine whether subjects can learn to switch among classes faster.

In the motor imagery session described in Figure 9, the subject was not able to properly rotate left. Inspecting Figure 11 explains why: during the baseline there was a large peak in the left-hand ROI, probably due to an artifact (such as hand motion instead of imagery). As a result, the baseline value for the left ROI was high. Since the current control paradigm is based on the percentage of signal change as compared to the baseline, it was difficult for the subject to exceed the high value of the baseline. In this particular session, the subject realized the limitation and was able to complete the task by turning almost 360° to the right instead of rotating left.

We are also interested in the subjective experience of the subjects: what is it like to control a robot by thought, using fMRI? The subjects filled in a questionnaire and were interviewed after most sessions. All subjects received the same questionnaire, which included 13 questions about their experience and control, such as "Was there a delay between thought and the avatar's movement?" and "Did you feel that the avatar was an

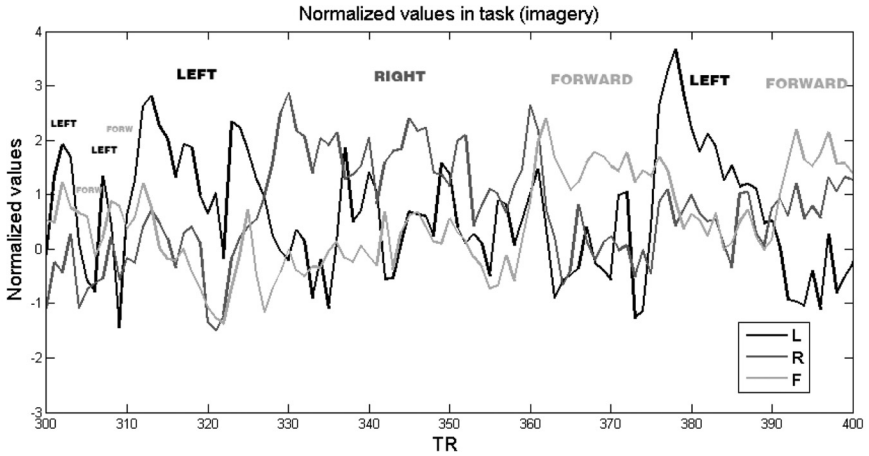


**Figure 9.** *Normalized activation levels of subject S1 in the three ROIs used to control the robot, during the task, using motor imagery.*

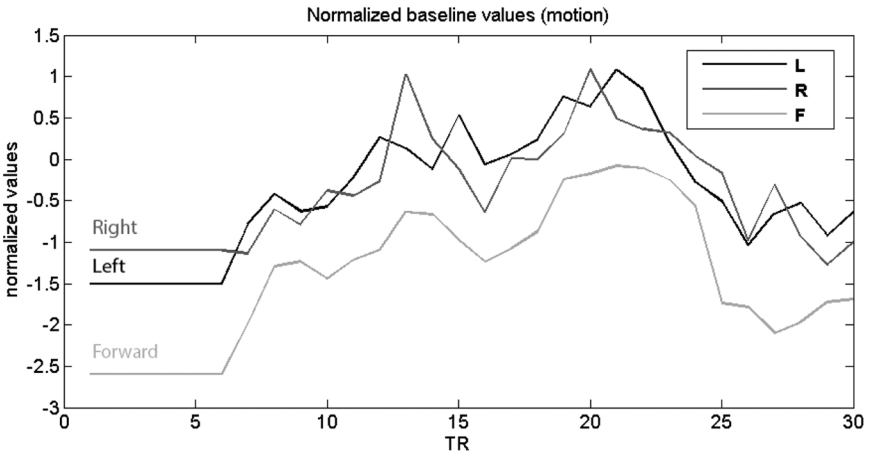


**Figure 10.** *Normalized activation levels of subject S1 in the three ROIs used to control the robot, during baseline, using motion.*

extension of your own body?" and "Did you feel that the avatar's right hand movement was an extension of your hand?" The small number of subjects does not allow for systematic analysis, but we can provide a few anecdotal comments. Subject S1 reported a strong sense of being in the robotic body and "in France." On one of the occasions, the technician picked the robot up in order to avoid hitting an obstacle, and S1 reported this as "hey, why is he lifting me up?" On another occasion we surprised S1 by introducing a mirror in the experiment room in France. The subject reported: "How cute, I have glowing eyes." Subject S2 reported that she felt "very small."

## 6 Conclusions and Future Work

The results of this study indicate that subjects can learn to control a robot using either motor imagery or movement, classified by our system, in better-than-chance levels with very little training. The system can also be used to train people for a BCI. Our aim is to allow subjects to perform diverse tasks in the virtual or real environment, using a natural mapping of mental patterns to functionality.

The ROI-based method we have presented here is simple and computationally efficient; we plan to extend it using machine learning techniques in order to iden-

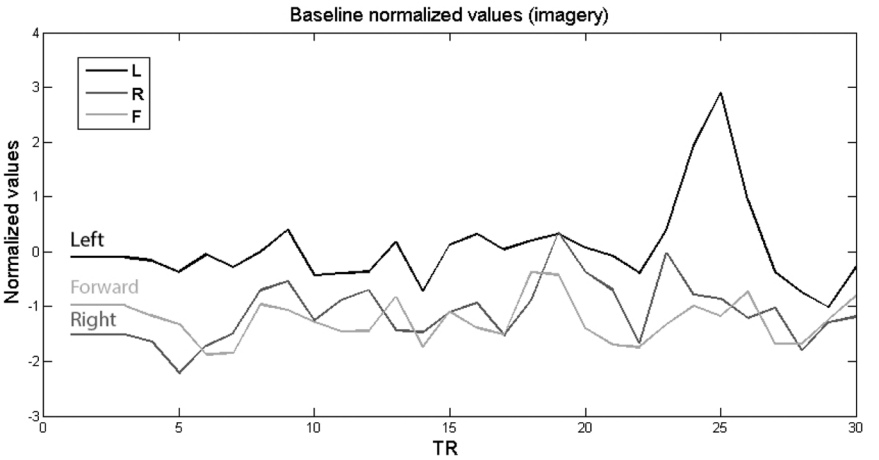


**Figure 11.** *Normalized activation levels of subject S1 in the three ROIs used to control the robot, during baseline, using motor imagery.*

tify more specific multivoxel brain patterns that may lead to identifying more complex intentions. In the course of these studies, we also intend to explore how the sensation of agency and embodiment develop in the context of such BCI experiences. This study is the first step and proves feasibility and potential; and we hope more exciting results will follow.

## Acknowledgments

This research is supported by the European Union FP7 Integrated Project VERE (No. 657295), www.vereproject.eu. We would like to thank the subjects for helping us. We would also like to thank Dan Drai, and the Weizmann's Institute technicians, Edna Furman-Haran, Nachum Stern, and Fanny Attar, for helping in this experiment.

## References

Bell, C. J., Shenoy, P., Chalodhorn, R., & Rao, R. P. N. (2008). Control of a humanoid robot by a noninvasive brain computer interface in humans. *Journal of Neural Engineering*, *5*(2), 214–220.

Cohen, O., Druon, S., Lengagne, S., Mendelsohn, A., Malach, R., Kheddar, A., & Friedman, D. (2012, June). fMRI robotic embodiment: A pilot study. *Biomedical Robotics and Biomechatronics* (pp. 314–319). IEEE Ras Embs International Conference. doi:10.1109/BioRob.2012.06290866

Cohen, O., Koppel, M., Malach, R., & Friedman, D. (2014). Controlling an avatar by thought using real-time fMRI. *Journal of Neural Engineering*, *11*(3), 035006.

deCharms, R. C. (2008). Applications of real-time fMRI. *Nature Reviews Neuroscience*, *9*(9), 720–729.

Donoghue, J. P., Nurmikko, A., Black, M., & Hochberg, L. R. (2007). Assistive technology and robotic control using motor cortex ensemble-based neural interface systems in humans with tetraplegia. *Journal of Physiology Special Issue on Brain Computer Interfaces*, *579*(3), 603–611.

Friedman, D., Leeb, R., Pfurtscheller, G., & Slater, M. (2010). Human–computer interface issues in controlling virtual reality with brain–computer interface. *Human–Computer Interaction*, *25*(1), 67–93.

Gergondet, P., Druon, S., Kheddar, A., Hintermuller, C., Guger, C., & Slater, M. (2011, December). Using brain-computer interface to steer a humanoid robot. *Proceedings of the IEEE International Conference on Robotics and Biomimetics, ROBIO*, 192–197.

Gergondet, P., Kheddar, A., Hintermuller, C., Guger, C., & Slater, M. (2012, June). Multitask humanoid control with a brain–computer interface: User experiment with HRP-2. *Proceedings of the 13th International Symposium on Experimental Robotics, ISER*.

Hochberg, L. R., Bacher, D., Jarosiewicz, B., Masse, N. Y., Simeral, J. D., Vogel, J., ... Donoghue, J. P. (2012). Reach and grasp by people with tetraplegia using a neurally controlled robotic arm. *Nature*, *485*(7398), 372–375.

Honryak, T. (2006). Thinking of child's play. *Scientific American*, *295*(3), 30. doi:10.1038/scientificamerican0906-30

Iturrate, I. N., Antelis, J. M., Kübler, A., & Minguez, J. (2009). A noninvasive brain-actuated wheelchair based on a P300 neurophysiological protocol and automated navigation. *Transactions on Robotics*, *25*(3), 614–627.

Kheddar, A. (2001). Teleoperation based on the hidden robot concept. *IEEE Transactions on Systems, Man, and Cybernetics, Part A*, *31*(1), 1–13.

Kim, S., Simeral, J. D., Hochberg, L., Donoghue, J., Friehs, G., & Black, M. (2011). A hybrid brain computer interface to control the direction and speed of a simulated or real wheelchair. *IEEE Transactions Neural Systems Rehabilitation Engineering*, *19*(2), 193–203.

Leeb, R., Friedman, D., Muller-Putz, G., Scherer, R., Slater, M., & Pfurtscheller, G. (2007). Self-paced (asynchronous) BCI control of a wheelchair in virtual environments: A case study with a tetraplegic. *Computational Intelligence and Neuroscience: Special Issue—Brain–Computer Interfaces: Towards Practical Implementations and Potential Applications.* doi:10.1155/2007/79642

Leeb, R., Keinrath, C., Friedman, D., Guger, C., Scherer, R., Neuper, C., ... Pfurtscheller, G. (2006). Walking by thinking: The brainwaves are crucial, not the muscles! *Presence: Teleoperators and Virtual Environments*, *15*(5), 500–514.

Lengagne, S., Ramdani, N., & Fraisse, P. (2011). Planning and fast replanning safe motions for humanoid robots. *IEEE Transactions on Robotics*, *27*(6), 1095–1106. doi:10.1109/TRO.2011.2162998

Lengagne, S., Vaillant, J., Yoshida, E., & Kheddar, A. (2013). Generation of whole-body optimal dynamic multi-contact motions. *International Journal of Robotics Research*, *32*(9–10), 1104–1119. doi:10.1177/0278364913478990

Lenhardt, A., & Ritter, H. (2010). An augmented-reality based brain–computer interface for robot control. In K. Wong, B. Mendis, & A. Bouzerdoum (Eds.), *Neural information processing: Models and applications. Lecture notes in computer science*, Vol. 6444 (pp. 58–65). Berlin: Springer-Verlag.

Leuthardt, E. C., Schalk, G., Wolpaw, J. R., Ojemann, J. G., & Moran, D. W. (2004). A brain–computer interface using electrocorticographic signals in humans. *Journal of Neural Engineering*, *1*(2), 63–71.

Mak, J. N., & Wolpaw, J. R. (2009). Clinical applications of brain–computer interfaces: Current state and future prospects. *IEEE Reviews in Biomedical Engineering*, *2*(1), 187–199. doi:10.1109/RBME.2009.2035356

Neuper, C., & Pfurtscheller, G. (2001). Event-related dynamics of cortical rhythms: Frequency-specific features and functional correlates. *International Journal of Psychophysiology*, *43*(1), 41–58.

Ortner, R., Guger, C., Prueckl, R., Graenbacher, E., & Edlinger, G. (2010). SSVEP based brain–computer interface for robot control. In K. Miesenberger, J. Klaus, W. Zagler, & A. Karshmer (Eds.), *Computers helping people with special needs. Lecture notes in computer science*, Vol. 6180 (pp. 85–90). Berlin: Springer-Verlag.

Pfurtscheller, G., Leeb, R., Keinrath, C., Friedman, D., Neuper, C., Guger, C., & Slater, M. (2006). Walking from thought. *Brain Research*, *1071*(1), 145–152.

Prueckl, R., & Guger, C. (2009). A brain–computer interface based on steady state visual evoked potentials for controlling a robot. In J. Cabestany, F. Sandoval, A. Prieto, & J. Corchado (Eds.), *Bio-inspired systems: Computational and ambient intelligence. Lecture notes in computer science*, Vol. 5517 (pp. 690–697). Berlin: Springer-Verlag.

Rebsamen, B., Burdet, E., Guan, C., Zhang, H., Teo, C. L., Zeng, Q., ... Laugier, C. (2006, February). A brain–controlled wheelchair based on P300 and path guidance. *Proceedings of the First IEEE/RAS-EMBS International Conference on Biomedical Robotics and Biomechatronics, BIOROB 2006*, 1101–1106. doi:10.1109/BIOROB.2006.1639239

Rebsamen, B., Guan, C., Zhang, H., Wang, C., Teo, C., Ang, M., & Burdet, E. (2010). A brain controlled wheelchair to navigate in familiar environments. *IEEE Transactions on Neural Systems Rehabilitation Engineering*, *18*(6), 590–598.

Royer, A. S., Doud, A. J., Rose, M. L., & He, B. (2010). EEG control of a virtual helicopter in 3-dimensional space using intelligent control strategies. *IEEE Transactions on Neural Systems Rehabilitation Engineering*, *18*(6), 581–589.

Sheridan, T. B. (1992). *Telerobotics: Automation and human supervisory control.* Cambridge, MA: MIT Press.

*Turbo Brainvoyager, Netherlands.* (n.d.). http://www.brainvoyager.com

Weiskopf, N., Mathiak, K., Bock, S. W., Scharnowski, F., Veit, R., Grodd, W., ... Birbaumer, N. (2004). Principles of a brain–computer interface (BCI) based on real-time functional magnetic resonance imaging (fMRI). *IEEE Transactions on Biomedical Engineering*, *51*(6), 966–970. Retrieved from http://ieeexplore.ieee.org/xpls/abs_all.jsp?arnumber=1300789

Weiskopf, N., Veit, R., Erb, M., Mathiak, K., Grodd, W., Goebel, R., & Birbaumer, N. (2003). Physiological self-regulation of regional brain activity using real-time functional magnetic resonance imaging (fMRI): Methodology and exemplary data. *NeuroImage*, *19*(3), 577–586. doi:10.1016/S1053-8119(03)00145-9